

Topological susceptibility in Lattice QCD with unimproved Wilson fermions

Abhishek Chowdhury, Asit K. De, Sangita De Sarkar, A. Harindranath*, Santanu Mondal, Anwesa Sarkar

*Theory Division, Saha Institute of Nuclear Physics
1/AF Bidhan Nagar, Kolkata 700064, India*

Jyotirmoy Maiti

*Department of Physics, Barasat Government College,
10 KNC Road, Barasat, Kolkata 700124, India*

Abstract

We address a long standing problem regarding topology in lattice simulations of QCD with unimproved Wilson fermions. Earlier attempt with unimproved Wilson fermions at $\beta = 5.6$ to verify the suppression of topological susceptibility with decreasing quark mass (m_q) was unable to unambiguously confirm the suppression. We carry out systematic calculations for two degenerate flavours at two different lattice spacings ($\beta = 5.6$ and 5.8). The effects of quark mass, lattice volume and the lattice spacing on the spanning of different topological sectors are presented. We unambiguously demonstrate the suppression of the topological susceptibility with decreasing quark mass, expected from chiral Ward identity and chiral perturbation theory.

Key words: Lattice QCD, Wilson fermions, chiral symmetry, topological charge, topological susceptibility

PACS: 11.15.-q, 11.15.Ha, 11.30.Rd, 12.38.-t, 12.38.Gc

1. Introduction

Because of the explicit violation of chiral symmetry by a dimension five kinetic operator, there have been persistent concerns about the Wilson formulation [1, 2] of fermions on the lattice in reproducing the chiral properties of continuum QCD. To address these concerns, for the past few years, we have been studying [3, 4] the chiral properties of Wilson lattice QCD. We have studied the emergence of the chiral anomaly

*Corresponding author

Email addresses: abhishek.chowdhury@saha.ac.in (Abhishek Chowdhury), asitk.de@saha.ac.in (Asit K. De), sangita.desarkar@saha.ac.in (Sangita De Sarkar), a.harindranath@saha.ac.in (A. Harindranath), santanu.mondal@saha.ac.in (Santanu Mondal), anwesa.sarkar@saha.ac.in (Anwesa Sarkar), jyotirmoy.maiti@gmail.com (Jyotirmoy Maiti)

with unimproved and improved Wilson fermions, the associated cutoff effects and the approach to the infinite volume chiral limit in the context of flavour singlet Axial Ward Identity to order $\mathcal{O}(g^2)$. In this work we address various issues associated with topological charge (Q) and topological susceptibility (χ) in lattice QCD simulations with two degenerate flavours of unimproved Wilson fermions. The detailed account of low lying spectroscopy and autocorrelation studies will appear separately.

Earlier attempt [5] with unimproved Wilson fermions and HMC algorithm performed simulation at $\beta = 5.6$, lattice volumes $16^3 \times 32$ and $24^3 \times 40$ and $m_\pi \geq 500$ MeV. Their results as well as the results from other collaborations [6] were presented, adopting a mass-dependent renormalization scheme, by scaling topological susceptibility and m_π^2 by appropriate powers of *quark mass dependent* r_0/a where r_0 is the Sommer parameter. Since r_0/a significantly increases with decreasing quark mass, the suppression of topological susceptibility may be concealed in such a plot especially for large pion masses and for lattice actions which have more severe cutoff artifacts. Results of Ref. [5] failed to show the suppression of topological susceptibility unambiguously when data was presented in this manner: see Fig.12 in Ref. [5]. (Note however that, at present, a mass-independent renormalization scheme appears to be preferred in the lattice literature where r_0 in the chiral limit is used to scale the data.) Since topological susceptibility is a measure of the spanning of different topological sectors of QCD vacuum, the inability to reproduce the predicted suppression may raise concerns about the simulation algorithm and the particular fermion formulation to span the configuration space correctly. Unimproved Wilson fermion has $\mathcal{O}(a)$ lattice artifact and hence it is also important to study the effects of scaling violation. We perform a systematic study using unimproved Wilson fermions at different volumes, different lattice spacings ($\beta = 5.6$ and 5.8) and $m_\pi \geq 300$ MeV. We present our data in both mass-dependent and mass-independent renormalization schemes. In the former scheme, our data (at both couplings $\beta=5.6$ and 5.8) clearly show the suppression of topological susceptibility in the region of pion mass $m_\pi \leq 500$ MeV. In the latter scheme, our data (at both couplings $\beta=5.6$ and 5.8) exhibit the suppression of topological susceptibility in the whole region of pion masses studied. When plotted using mass independent scheme, the data of Ref. [5] also clearly show the suppression of topological susceptibility for the available range of their data ($m_\pi \geq 500$ MeV). Since our data exhibits suppression in the lower pion mass region *independent of the renormalization scheme used*, we are able to demonstrate *unambiguously* the suppression of topological susceptibility with decreasing quark mass, expected in continuum QCD in the region of lower pion mass. Advancements in both algorithm and technology have made this study possible.

2. Measurements

We have generated ensembles of gauge configurations by means of HMC [7, 8] and DDHMC [9] algorithm using unimproved Wilson fermion and gauge actions with $n_f = 2$ mass degenerate quark flavours. At $\beta = 5.6$ the lattice volumes are $16^3 \times 32$, $24^3 \times 48$ and $32^3 \times 64$ and the renormalized physical quark mass (calculated using axial Ward identity) ranges between 15 to 100 MeV ($\overline{\text{MS}}$ scheme at 2 GeV). At $\beta = 5.8$ the lattice volume is $32^3 \times 64$ and the renormalized physical quark mass ranges from 20 to

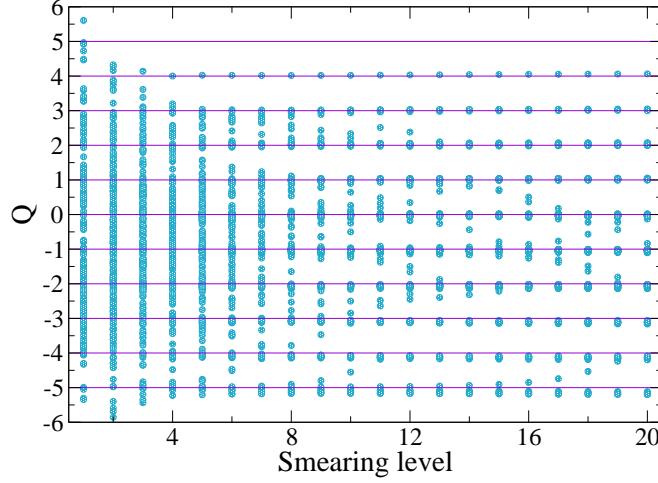


Figure 1: Topological charge of gauge configurations versus HYP smearing steps for $\beta = 5.8$ and $\kappa = 0.15475$ ($m_\pi \sim 300\text{MeV}$) at lattice volume $32^3 \times 64$.

90 MeV. The lattice spacings determined using Sommer parameter at $\beta = 5.6$ and 5.8 are 0.077 and 0.061 fm respectively. The configurations for lattice volumes $24^3 \times 48$ and $32^3 \times 64$ and for $16^3 \times 32$ at $\kappa = 0.15775$ are generated using DDHMC algorithm. The number of thermalized configurations ranges from 2000 to 12000 and the number of measured configurations ranges from 70 to 500.

For topological charge density, we use the lattice approximation developed for $SU(2)$ by DeGrand, Hasenfratz and Kovacs [10], modified for $SU(3)$ by Hasenfratz and Nietner [11] and implemented in the MILC code [8]. It uses ten link paths described by unit lattice vector displacements in the sequence $\{x, y, z, -y, -x, t, x, -t, -x, -z\}$ and $\{x, y, z, -x, t, -z, x, -t, -x, -y\}$ plus rotations and cyclic permutations. To suppress the ultraviolet lattice artifacts, smearing of link fields is required. The link field is smeared by 20 HYP smearing steps and optimized smearing coefficients $\alpha = 0.75$, $\alpha_2 = 0.6$ and $\alpha_3 = 0.3$ [12]. We have observed that smearing brings the topological charges close to integer values and behaviour is better for the smaller lattice spacing, as expected.

In Fig. 1 we show the behaviour of topological charge of gauge configurations with smearing steps for $\beta = 5.8$ and $\kappa = 0.15475$ at lattice volume $32^3 \times 64$. It is evident that the topological charges of different configurations are clustering about the integer values after about 10 smearing steps and values are stable under further smearing steps. In Fig. 2 we present the behaviour of topological susceptibility with smearing steps for the same lattice parameters which shows that the susceptibility is very stable with smearing steps after 10 steps.

In Fig. 3 we show the Monte Carlo time history of topological charge for $\beta = 5.6$ and 5.8 for the smallest and the largest κ and there is some evidence of trapping of the

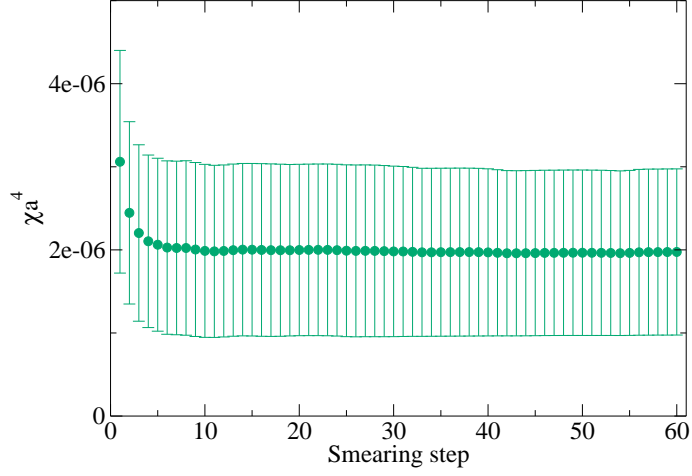


Figure 2: Topological susceptibility versus HYP smearing steps for $\beta = 5.8$ and $\kappa = 0.15475$ at lattice volume $32^3 \times 64$.

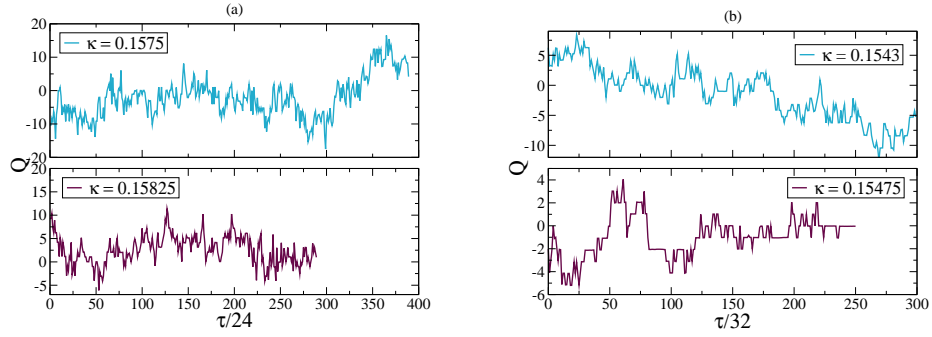


Figure 3: The Monte Carlo trajectory history for topological charge with unimproved Wilson fermion and gauge action for (a) $\beta = 5.6$ with a gap of 24 trajectories between two consecutive measurements and (b) $\beta = 5.8$ with a gap of 32 trajectories between two consecutive measurements.

topological charge only at $\beta = 5.8$ and largest κ .

Fig. 4 displays six histograms of topological charge distributions, for two values of β and different volumes. The topological charge data were put in several bins and the bin widths were chosen to be unity centered around the integer values of the topological charges for all the cases. From theoretical considerations the distribution of the topological charge is expected to be a Gaussian [13]. Since our configurations are large in number but finite, an incomplete spanning of the topological sectors may occur and $\langle Q \rangle$ may not be zero. Hence we define the susceptibility to be

$$\chi = \frac{1}{V} (\langle Q^2 \rangle - \langle Q \rangle^2). \quad (1)$$

The expected distribution is

$$n_Q = \frac{n_{meas}}{\sqrt{2\pi(\langle Q^2 \rangle - \langle Q \rangle^2)}} \exp\left(-\frac{Q^2}{2(\langle Q^2 \rangle - \langle Q \rangle^2)}\right) \quad (2)$$

where n_{meas} is the total number of measurements made. The Gaussian curves in Fig. 4 are obtained by using Eq. 2. It is evident from Fig. 4 that for a given β and volume the width of the distribution decreases as κ increases, indicating that the topological susceptibility χ decreases with decreasing quark mass.

3. Results

In table 1 we present, in lattice units, the pion masses, unrenormalized quark masses and topological susceptibilities measured. For ease of comparison with earlier presentations of results and clarification we present for $\beta = 5.6$ and 5.8 at lattice volume $32^3 \times 64$, topological susceptibility versus m_π^2 in the units of r_0 (quark mass dependent), (i.e., in mass-dependent renormalization scheme) in Fig. 5. At $\beta = 5.6$ our second largest quark mass (in Fig. 5) is very close to the lowest quark mass of Ref. [5]. In this figure the shaded region corresponds to $m_\pi \geq 500$ MeV. In the lower pion mass region our data for both $\beta = 5.6$ and 5.8 clearly show the suppression even in mass-dependent renormalization scheme.

Fig. 6 shows our results for topological susceptibility versus m_π^2 , in the units of Sommer parameter (r_0) at the chiral limit (i.e., in the mass-independent renormalization scheme), for $\beta = 5.6$ and at lattice volumes $16^3 \times 32$, $24^3 \times 48$, and $32^3 \times 64$. We also show the results of SESAM-T χ L collaborations [5]. Using the numbers given in [5], we have replotted it after scaling by the value of r_0 quoted at the physical point. This new plot clearly shows the suppression of susceptibility with decreasing quark mass in the earlier SESAM-T χ L data with unimproved Wilson fermion. Our results carried out at larger volume and smaller quark masses unambiguously (i.e., independent of the renormalization schemes used) establish the suppression of topological susceptibility with decreasing quark mass in accordance with the chiral Ward identity and chiral perturbation theory. Further we note that, for a given κ , the value of topological susceptibility increases with the volume as expected from finite volume considerations. This effect is more noticeable in smaller volumes. For large enough volume topological susceptibility should be independent of volume, since $\langle Q^2 \rangle$ scales with the volume.

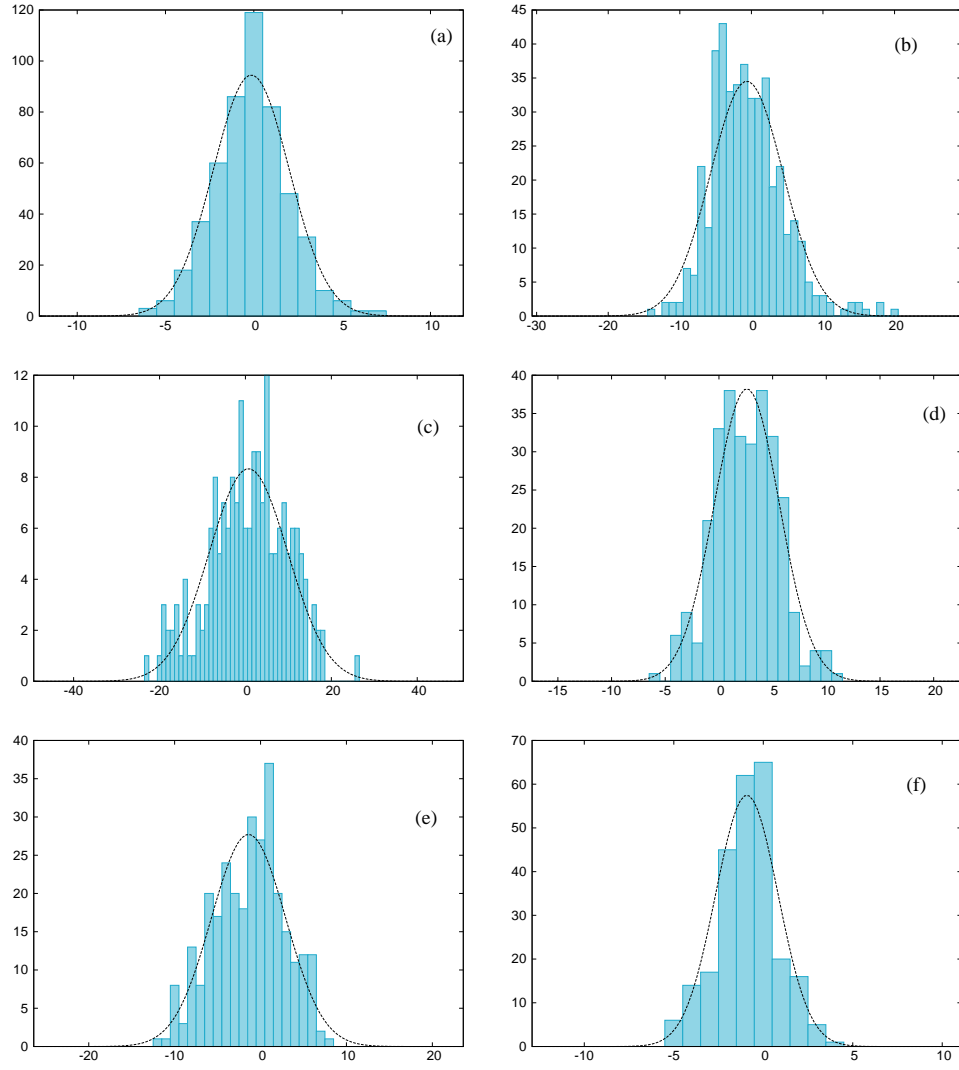


Figure 4: The topological charge distribution for (a) $\beta = 5.6$, $\kappa = 0.15775$, volume = $16^3 \times 32$ (b) $\beta = 5.6$, $\kappa = 0.15775$, volume = $24^3 \times 48$ (c) $\beta = 5.6$, $\kappa = 0.15775$, volume = $32^3 \times 64$ (d) $\beta = 5.6$, $\kappa = 0.15825$, volume = $24^3 \times 48$ (e) $\beta = 5.8$, $\kappa = 0.1543$, volume = $32^3 \times 64$ (f) $\beta = 5.8$, $\kappa = 0.15475$, volume = $32^3 \times 64$.

$\beta = 5.6$					
	<i>lattice</i>	κ	am_π	am_q	$\chi a^4/10^{-5}$
	$16^3 \times 32$	0.156	0.4456(19)	0.06724(78)	11.9020(1.255)
	,,	0.157	0.3441(27)	0.04004(61)	7.6147(0.948)
	,,	0.1575	0.2867(27)	0.02813(57)	5.6381(0.863)
	,,	0.15775	0.2529(28)	0.02018(50)	3.6700(0.919)
	,,	0.158	0.2258(35)	0.01388(48)	2.9405(0.354)
	$24^3 \times 48$	0.1575	0.2717(15)	0.02669(37)	5.4727(1.56)
	,,	0.15775	0.2387(21)	0.02127(37)	3.8986(0.764)
	,,	0.158	0.1967(24)	0.01441(29)	3.9070(0.800)
	,,	0.158125	0.1767(23)	0.01143(22)	2.6140(1.30)
	,,	0.15825	0.1478(24)	0.00690(17)	1.3804(0.646)
	$32^3 \times 64$	0.15775	0.2359(16)	0.02042(29)	3.9826(0.574)
	,,	0.158	0.1979(16)	0.01489(32)	3.5056(0.775)
	,,	0.15815	0.1669(17)	0.01070(19)	2.4784(0.829)
	,,	0.1583	0.1301(20)	0.00632(18)	1.4420(0.678)
$\beta = 5.8$					
	<i>lattice</i>	κ	am_π	am_q	$\chi a^4/10^{-5}$
	$32^3 \times 64$	0.1543	0.1585(11)	0.01338(14)	0.8891(0.248)
	,,	0.15455	0.1228(10)	0.00767(9)	0.3704(0.144)
	,,	0.15475	0.0920(23)	0.00365(11)	0.1447(0.087)

Table 1: Pion masses, unrenormalized quark masses and topological susceptibilities in lattice units.

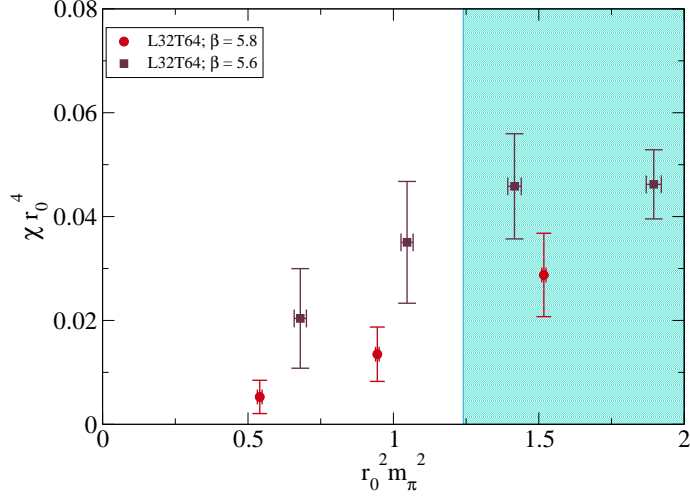


Figure 5: Topological susceptibility versus m_π^2 in the units of r_0 (quark mass dependent) for $\beta = 5.6$ and 5.8 and at lattice volume $32^3 \times 64$.

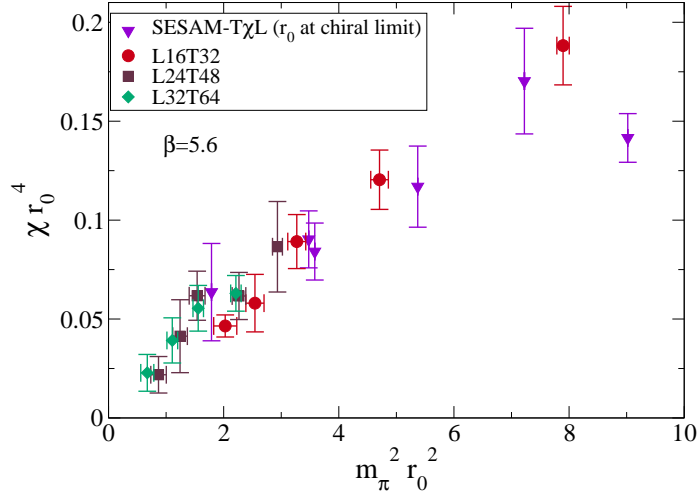


Figure 6: Topological susceptibility versus m_π^2 in the units of r_0 (at chiral limit) for $\beta = 5.6$ and at lattice volumes $16^3 \times 32$, $24^3 \times 48$, and $32^3 \times 64$ compared with the results of SESAM-TchiL collaborations [5].

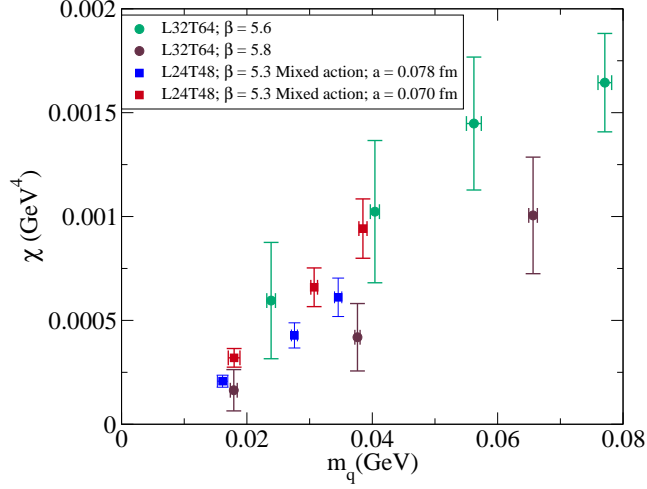


Figure 7: Topological susceptibility versus m_q in the physical units for $\beta = 5.6$ and $\beta = 5.8$ at lattice volume $32^3 \times 64$ compared with the results of mixed action (Clover and Overlap) [18]. For the latter, the two separate lattice spacing determinations, $a = 0.0784$ fm and $a = 0.070$ fm quoted have been used.

Since unimproved Wilson fermion has $\mathcal{O}(a)$ lattice artifacts it is important to estimate the scaling violations of our results. Fig. 7 shows topological susceptibility in the physical units for $\beta = 5.6$ and $\beta = 5.8$ at lattice volume $32^3 \times 64$ versus nonperturbatively renormalized [14] quark mass in $\overline{\text{MS}}$ scheme [15] at 2 GeV. Topological susceptibility at $\beta = 5.8$ approximately matches with that at $\beta = 5.6$ within the error bars but the latter data is systematically below the former. This behaviour which is qualitatively consistent with leading order lattice artifact [16] is observed also by the MILC collaboration [17]. For comparison, in Fig. 7, we have also shown the results of mixed action calculation of Ref. [18] at $\beta = 5.3$ where the authors have quoted two separate lattice spacings, $a = 0.0784$ fm and $a = 0.070$ fm for the same β . The calculation of Ref. [18] employs gauge configurations generated with dynamical $\mathcal{O}(a)$ improved Wilson fermion, using DDHMC algorithm and topological charge is measured using a fermionic operator, namely, the Neuberger-Dirac operator. Fig. 7 shows that our results of the topological susceptibility favourably compare with that of Ref. [18]. In Ref. [19] we have shown that (see Fig. 6 of Ref. [19]) the topological susceptibility at $\beta = 5.8$ is consistent with leading order chiral perturbation theory prediction.

In conclusion, we have addressed a long standing problem regarding topology in lattice simulations of QCD with unimproved Wilson fermions. Calculations are presented for two degenerate flavours. The effects of quark mass, lattice volume and the lattice spacing on the spanning of different topological sectors are presented. By performing simulations at smaller pion masses we have shown the suppression of the topological susceptibility with respect to decreasing quark mass irrespective of the method

of presenting the data. The suppression expected from chiral Ward identity and chiral perturbation theory is thus demonstrated unambiguously. Furthermore, our results of the topological susceptibility favourably compare with that of $\mathcal{O}(a)$ improved Wilson fermion. Our results unequivocally show that lattice QCD with naive Wilson fermions together with DDHMC algorithm, for the range of quark masses and lattice spacings studied, is able to span the configuration space correctly and reproduce the chiral behaviour of continuum QCD. In future work, we would like to explore lighter quark masses and smaller lattice spacings. To achieve this goal, however, improvements in the algorithm might be necessary.

Acknowledgements

Numerical calculations are carried out on Cray XD1 and Cray XT5 systems supported by the 10th and 11th Five Year Plan Projects of the Theory Division, SINP under the DAE, Govt. of India. We thank Richard Chang for the prompt maintenance of the systems and the help in data management. This work was in part based on the public lattice gauge theory codes of the MILC collaboration [8] and Martin Lüscher [9].

References

- [1] K. G. Wilson, Phys. Rev. **D10**, 2445-2459 (1974).
- [2] K. G. Wilson, “Quarks and Strings on a Lattice”, in *New Phenomena in Sub-nuclear Physics*, Proceedings of the International School of Subnuclear Physics, Erice, 1975, edited by A. Zichichi (Plenum, New York, 1977).
- [3] A. K. De, A. Harindranath and S. Mondal, Phys. Lett. B **682**, 150 (2009) [arXiv:0910.5611 [hep-lat]].
- [4] A. K. De, A. Harindranath and S. Mondal, JHEP **1107**, 117 (2011) [arXiv:1105.0762 [hep-lat]].
- [5] G. S. Bali *et al.* [SESAM and T χ L Collaborations], Phys. Rev. **D64**, 054502 (2001). [hep-lat/0102002].
- [6] See for examples, S. Durr, Nucl. Phys. **B611**, 281-310 (2001), [hep-lat/0103011]; A. Hasenfratz, Phys. Rev. D **64**, 074503 (2001) [arXiv:hep-lat/0104015].
- [7] S. Duane, A. D. Kennedy, B. J. Pendleton, D. Roweth, Phys. Lett. **B195**, 216 (1987).
- [8] <http://physics.indiana.edu/~sg/milc.html>
- [9] M. Lüscher, Comput. Phys. Commun. **156**, 209-220 (2004). [hep-lat/0310048]; M. Lüscher, Comput. Phys. Commun. **165**, 199-220 (2005). [hep-lat/0409106]. <http://luscher.web.cern.ch/luscher/DD-HMC/index.html>
- [10] T. A. DeGrand, A. Hasenfratz, T. G. Kovacs, Nucl. Phys. **B505**, 417-441 (1997). [arXiv:hep-lat/9705009 [hep-lat]].
- [11] A. Hasenfratz, C. Nieter, Phys. Lett. **B439**, 366-372 (1998). [hep-lat/9806026].

- [12] A. Hasenfratz, F. Knechtli, Phys. Rev. **D64**, 034504 (2001). [hep-lat/0103029].
- [13] H. Leutwyler, A. V. Smilga, Phys. Rev. **D46**, 5607-5632 (1992); A. S. Hassan, M. Imachi, N. Tsuzuki, H. Yoneyama, Prog. Theor. Phys. **94**, 861-872 (1995), [hep-lat/9508011]; S. Durr, Nucl. Phys. **B611**, 281-310 (2001), [hep-lat/0103011]; R. Brower, S. Chandrasekharan, J. W. Negele, U. J. Wiese, Phys. Lett. **B560**, 64-74 (2003), [hep-lat/0302005]; L. Giusti, M. Luscher, P. Weisz, H. Wittig, JHEP **0311**, 023 (2003), [hep-lat/0309189]; S. Aoki, H. Fukaya, S. Hashimoto, T. Onogi, Phys. Rev. **D76**, 054508 (2007), [arXiv:0707.0396 [hep-lat]].
- [14] D. Becirevic, B. Blossier, P. Boucaud, V. Gimenez, V. Lubicz, F. Mescia, S. Simula, C. Tarantino, Nucl. Phys. **B734**, 138-155 (2006). [hep-lat/0510014].
- [15] V. Gimenez, L. Giusti, F. Rapuano, M. Talevi, Nucl. Phys. **B540**, 472-490 (1999). [hep-lat/9801028].
- [16] P. Di Vecchia, K. Fabricius, G. C. Rossi and G. Veneziano, Nucl. Phys. B **192**, 392 (1981).
- [17] A. Bazavov *et al.* [MILC Collaboration], Phys. Rev. **D81**, 114501 (2010). [arXiv:1003.5695 [hep-lat]].
- [18] F. Bernardoni, P. Hernandez, N. Garron, S. Necco, C. Pena, Phys. Rev. **D83**, 054503 (2011). [arXiv:1008.1870 [hep-lat]].
- [19] A. Chowdhury, A. K. De, S. De Sarkar, A. Harindranath, S. Mondal, A. Sarkar and J. Maiti, arXiv:1111.1812 [hep-lat].